LBL-31581

Lawrence Berkeley Laboratory
UNIVERSITY OF CALIFORNIA

ENERGY & ENVIRONMENT DIVISION

To be presented at the Spring Meeting of the Western States Section of the Combustion Institute, Corvalis, OR, March 23–24, 1992, and to be published in the Proceedings

Freely Propagating Open Premixed Turbulent Flames Stabilized by Swirl

C.K. Chan, K.S. Lau, W.K. Chin, and R.K. Cheng

December 1991

ENERGY & ENVIRONMENT DIVISION

LOAN COPY
Circulates
for 4 weeks
Bldg. 50 Library.
LBL-31581
Copy 2

Prepared for the U.S. Department of Energy under Contract Number DE-AC03-76SF00098

DISCLAIMER

This document was prepared as an account of work sponsored by the United States Government. While this document is believed to contain correct information, neither the United States Government nor any agency thereof, nor the Regents of the University of California, nor any of their employees, makes any warranty, express or implied, or assumes any legal responsibility for the accuracy, completeness, or usefulness of any information, apparatus, product, or process disclosed, or represents that its use would not infringe privately owned rights. Reference herein to any specific commercial product, process, or service by its trade name, trademark, manufacturer, or otherwise, does not necessarily constitute or imply its endorsement, recommendation, or favoring by the United States Government or any agency thereof, or the Regents of the University of California. The views and opinions of authors expressed herein do not necessarily state or reflect those of the United States Government or any agency thereof or the Regents of the University of California.

LBL-31581

Freely Propagating Open Premixed Turbulent Flames Stabilized by Swirl

C.K. Chan, K.S. Lau, and W.K. Chin

Hong Kong Polytechnic
Hong Kong

and

R.K. Cheng

Combustion Group
Energy and Environment Division
Lawrence Berkeley Laboratory
University of California
Berkeley, California 94720

December 1991

This work was supported in part by a Research and Development Grant from the Hong Kong Polytechnic and by the Director, Office of Energy Research, Office of Basic Energy Sciences, Chemical Sciences Division, of the U.S. Department of Energy under Contract No. DE-AC03-76SF00098.

ABSTRACT

A novel means has been developed for using weak swirl to stabilize freely propagating open premixed turbulent flames (swirl numbers between 0.05 to 0.3). By injecting a small amount of air tangentially into the co-flow of a concentric burner, stationary flames can be maintained above the burner exit for a large range of mixture, turbulence and flow conditions. The absence of physical surfaces in the vicinity of the flame provides free access to laser diagnostics. Laser Doppler anemometry and laser Mie scattering measurements of four flames with and without incident turbulence show that their features are typical of wrinkled laminar flames. The most distinct characteristics is that flame stabilization does not rely on flow recirculation. Centrifugal force induced by swirl causes flow divergence, and the flame is maintained at where the local mass flux balances the burning rate. The flame speeds can be estimated based on the centerline velocity vector, which is locally normal to the flame brush. This flame geometry is the closest approximation to the 1-D planar flame for determining fundamental properties to advance turbulent combustion theories.

Introduction

Flame stabilization by swirl is a common feature of many turbines and furnaces. Varying the degree of swirl provides the control of their operation over a large range of conditions. Many fundamental aspects of the complex interaction between swirl and non-premixed flames[1-6], premixed flames[7-9] and spray combustion[10,11] have been investigated experimentally in laboratories using turbine and furnace simulators. Theoretical models have also been developed to predict combustor performance and other characteristics [e.g. 9]. The most distinct flowfield feature is the large recirculation or toroidal vortex which is vital to steady operation. Because all swirl combustors are enclosed, there have been relatively few studies of open swirl stabilized flames.

Starner and Bilger[4] investigated a non-premixed turbulent jet flame interacting with weak co-flow swirl. They argued that much can be learned from the unconfined system because it is more accessible to probing by laser diagnostics. Their results show that swirl shortens the flame. This shortening is attributed to swirl-induced radial pressure gradients. Many features of their results, however, are similar to those of non-swirl flames. For flames with intense swirl where the recirculation zone becomes predominant, recent investigations have focused on studying the influence of recirculation on blowout and stability limits[5,6]. For premixed flames, the significance of the recirculation zone on open and enclosed systems has also been addressed by many investigators[7-9]. Syred and Beer[2] described their very rich ($1.2 < \phi < 6.0$) open flame as noisy and unstable. Fujii et al.[7] reported that the flowfield of the unconfined annular swirl burner was drastically altered by combustion.

For our study of the effect of swirl on open premixed turbulent flames, we have chosen a configuration which is a modification of the premixed flame burner used in previous studies[12]. It consists of a central flow of premixed fuel/air surrounded by co-flow air.

Swirl is generated by tangential air injection which is one of the classical swirl generators suggested by Beer and Chigier[1]. This flow arrangement is similar to that of the enclosed premixed swirl burner used in the study of Gouldin et al.[8] For conditions of weak swirl, we have found that it provides a novel means of stabilizing freely propagating yet steady premixed flames which maintain at a distance above the burner exit (Fig. 1). This interesting and useful phenomenon of flame stabilization by swirl has yet to be reported in the literature. The flame flowfield is not influenced by physical boundaries, as in the cases of stagnation point flames, rod-stabilized v-flames and Bunsen flames. It gives free access to laser diagnostics and has the potential of being one of the most ideally suited configurations for investigating fundamental properties of premixed turbulent flames.

The objective of this paper is to characterize the freely propagating premixed flames stabilized by weak swirl. The non-reacting and reacting flowfields with and without incident turbulence are investigated using two-component laser Doppler anemometry (LDA) which measures velocity statistics, and Mie scattering from oil droplets (MSOD) technique which infers the scalar statistics. The results are analyzed using well-established procedures for premixed turbulent flames to elucidate the stabilization mechanism, and for comparison with those obtained in other configurations. Our investigation shows that even though swirl is vital to stabilizing the steady flame, the flame zone and its properties are not affected by shear associated with swirl. Consequently, this flame configuration is the closest approximation, to date, to the planar one-dimensional premixed turbulent flame of many theoretical models. It is also capable of stabilizing flames at a much wider range of equivalence ratio and should be further exploited experimentally and theoretically to advance fundamental research on premixed turbulent flame propagation.

Experimental Setup

The schematic of the swirl burner and the experimental setup is shown in Figure 2. The burner is supplied by a 50 mm diameter inner core of fuel/air mixture surrounded by an annular co-flow air jet of 114 mm diameter. Swirl is generated by injecting air tangentially through two tangential air inlets of 6.1 mm diameter. As the air supply to the tangential inlets is independent of the co-flow air supply, a range of swirl numbers, S, is obtained by adjusting the tangential air flow which is monitored by a rotameter. A turbulence grid with 5 mm grid spacing and a perforated plate with 4.76 mm diameter holes 1.8 mm apart are used to generate incident turbulence. The turbulence intensities generated, as reported by Cheng and Ng,[13] are between 5 and 8.5%.

Velocity measurements are made using a four-beam 2-color LDA system[12]. The fringe spacings for the beam intersections are 2.42 μm and 2.56 μm for axial and transverse velocities, respectively. The laser, transmitting and receiving optics are mounted on a computer controlled 3-axis traversing table. A differential frequency shift of 5 MHz is imposed on the transverse velocity component to remove directional ambiguity. The Doppler signals are analyses by two TSI frequency counters interfaced with and controlled by a 80386 PC. 4096 samples are used in the on-line and off-line computation

of the co-validated signals. The co-validation criterion is 10μsec. Alumina particles of nominal size of 0.3μm are used as LDA seeds for the fuel/air flow while a silicon oil aerosol provides the seeds for the co-flow and the swirl injectors. Profiles of radial velocity components, V, and the tangential velocity component, W, are obtained by traversing the laser probe on the planes perpendicular (x-y) and parallel (x-z) to the laser direction (z), respectively. Flowline tracing[14] to map flow divergence is obtained on the x-y plane. Data reduction is performed in the way as described previously[12].

Reaction progress variable, c, and flame crossing frequency, ν, are measured by means of MSOD. This technique[14] was found to be very convenient for mapping the flame boundaries. Mie scattering from the 488 nm beams is collected by a photomultiplier assembly focused at the beam intersection, then digitized using a A/D converter. The reaction progress variable, c, which varies from 0 in the reactants to 1 in the products and the flame crossing frequency, ν, are deduced by assigning a threshold to discriminate between the contributions from reactant and product states[14].

The swirl number, S, for this configuration is given by Beer and Chigier[1], and is the ratio of axial flux of angular momentum to axial flux of linear momentum divided by the burner radius. Claypole and Syred[3] have shown that S can be conveniently obtained from the burner geometry and mass flow rate by

$$S_1 = \frac{\pi r_0 R}{A_t} \left(\frac{m_\theta}{m_\theta + m_A}\right)^2 \tag{1}$$

where r_0 is the radius of the tangential inlet, R is the radius of the burner, A_t is the total area of the tangential air inlets, m_θ and m_A are the tangential and axial mass flow rates respectively.

Experimentally, it has been shown [5-7] that S can be obtained more appropriately as

$$S_2 = \frac{\int_0^\infty UWr^2 dr}{R\int_0^\infty (U^2 - \frac{W^2}{2})\, r\, dr} \tag{2}$$

Metering the volumetric rate of the tangential injections and measuring U and W provide independent means to determine the swirl number from Equation (1), S_1 , and Equation (2), S_2.

Results and Discussion

Initially, lighting the flame involves using a small blunt body as the flame stabilizer suspended at the end of a thin rod. Before turning on the swirl injectors, an inverted conical flame (see schlieren record of ref. 13) can be stabilized at the center of the burner. The introduction of swirl opens the flame. With increasing swirl, the flame begins to detach from the blunt body indicating that freely propagating conditions has been reached and the blunt body can be removed. It was found later that once these conditions are set, the flame can be re-lit without using the blunt body. Figure 1 shows two identical flames with and without the turbulence generator (SWF1 and SWF2 of Table I). The flame brush is more planar for SWF1 and, as expected, the curved turbulent SWF2 flame brush is thicker. The slight asymmetry of SWF2 is probably due to an imbalance of the two tangential air inlets. Clogging of the screens inside the flow settling chamber could also cause gross asymmetry of the flame brush. Because the flame are stabilized by fluid mechanical means, they are very sensitive to changes in flow conditions. SWF1 is found to bounce and the flame sheet is not completely free of wrinkles as expected of a laminar flame. The bouncing movement is probably caused by perturbations of the swirl air supply.

Table I Experimental Conditions

Case	Turb. source	Fuel	ϕ	S_1	S_2	v_{max} at x =0.0	u'/S_l	S_t/S_l	Symbol
Flow 1	none	none	0.0	0.07	0.18	-	-	-	■
Flow 2	plate	none	0.0	0.07	0.13	-	-	-	◆
SWF1	none	C_2H_4	0.65	0.07	0.13	20	0.26	1.51	+
SWF2	plate	C_2H_4	0.65	0.07	0.12	90	1.0	4.0	∇
SWF3	plate	CH_4	0.8	0.08	0.12	120	1.33	4.67	×
SWF4	grid	CH_4	1.0	0.07	0.12	100	0.63	3.33	Δ

A parametric study was carried out to determine the stabilization range by varying the tangential injection rate, the co-flow rate, and the equivalence ratio, ❊, and by the use of different turbulence generators including a square grid and two perforated plates[13]. To be compatible with the conditions of previous v-flames and stagnation point flames[14], the exit velocity of the flow without swirl was maintained at 5.0 m/s equal to a Reynolds number, Re, of 40,000 based on the burner diameter. Using a C_2H_4 /air mixture of ϕ = 0.75, it was found that varying swirl changes the position of the flame brush. Weaker swirl pushes the flame downstream until the flame blows off. Stronger swirl pulls the flame closer to the exit and into the straight section. The overall range of swirl number, S_1, which supports steady turbulent flame operation is from 0.05 to 0.38. The range is narrower without turbulence ($0.05 < S_1 < 0.3$). These swirl numbers are significantly lower than those reported in other studies of open and enclosed swirl flames. The lean stabilization limit determined for methane/air mixtures with S_1 at 0.07 is ❊ = 0.57. This

lean limit is the lowest compared to those of other laboratory flame configurations[12]. In general, changing the co-flow rate does not seem to have a significant effect on the stabilization range, nor on the flame shape, while keeping the fuel/air mixture constant. Consequently, all detailed studies were performed with the co-flow velocity matching that of the core.

The experimental conditions with Re = 40,000 chosen for detail measurements are listed in Table I. Figure 3 shows the mean radial V(r) and tangential W(r) velocity profiles at 10 mm above the exit. Measurement closer than 10 mm is not possible because one of the laser beams is blocked by the burner rim. The V(r) profiles are all linear within the fuel/air core with zero crossing points close to the center, which indicates that the swirl generated flowfield is divergent. The strain rate dV(r)/dr averaged about 25 (1/sec.), which is about 20% of typical stagnation point flames condition[12].

Due to the constraints of the laser table, the measurement domain on the x-z plane, i.e. w(r), is confined to $-30 < r < 60$ mm. The most striking feature is that swirling motion is only significant outside the 25 mm diameter fuel/air core. Despite the fact that the flame is stabilized by swirl, the tangential component of velocity component across the reaction zone is negligible, which indicates that the flame zone is in fact free of the influence of swirl. The values of S_2 (from Eq. 2) deduced from these profiles are listed in Table I. It is clear that S_2 are higher than S_1. The difference demonstrates the problem with applying Eq. 2 to open systems. Unlike enclosed swirling flows, open systems have no clearly defined outer boundary for the integration. These values of S_2 are deduced by integrating from r = 0 to the burner rim where, as seen in Fig. 3(b), W is still increasing.

The centerline mean axial velocity U(x) profiles of Fig. 4(a) show that swirl reduces the centerline velocity from 5.0 to below 2.0 m/s near the exit. For non-reacting Flow 1 and Flow 2, the gradual decrease indicates flow divergence which is also shown by the V(r) profiles in Fig 3(a). These U(x) profiles clearly demonstrate that recirculation is not present and therefore, not relevant to flame stabilization. The flame zones of SWF1 through SWF4 are marked by the increases in U(x) caused by combustion-induced acceleration. This increase is characteristics of premixed turbulent flames under similar flow and mixture conditions. SWF3 demonstrates that a small increase in swirl draws the flame zone closer to the exit. Downstream from the flame zone, the profiles show gradual decreases. These changes are small compared to those observed in v-flames where the product flow accelerates, or in stagnation flow stabilized flames where the product flow decelerates.

Within the flame zones, the MSOD signals resemble telegraph signals generated by wrinkled flamelets. The flame crossing frequency, ν, then indicates the mean time scale of the wrinkles. As shown in Table I, SWF1 has the lowest ν. Because SWF1 does not use a turbulence generator, its ν is most likely associated with the perturbation frequency of the swirl injectors. The values of ν obtained for SWF2 to SWF4 are about four to six times higher, and are compatible with those observed in the stagnation point flames. It is also interesting to note that the turbulent flames SWF2 - 4 do not bounce and have

typical wrinkled laminar flame appearance, which shows that small scale turbulence tends to damp out low frequency effects.

In Fig. 4(b) the non-reacting u'(x) profiles remain constant. The lack of turbulence decay is a feature of strained turbulent flowfields as in the case of stagnation point flows[15]. For SWF1 through SWF4, u' peaks at the flame zone. Downstream of the flame brush an increase in u' compared to incident turbulence intensity is observed only for SWF1 and SWF4, both with lower incident turbulence.

As shown in the contour plot of Fig. 5, the velocity joint probability density function (jpdf) at the peak near c = 0.5 is bi-modal indicating again typical wrinkled flamelet characteristics. The separation between the two peaks (i.e. islands on the contour plot) represents the mean flow acceleration across the flamelet, which is the main contributor to the u' peak. Flame-generated turbulence can also be inferred from the jpdf by deducing the conditioned velocity statistics using the same procedure described by Cheng[16]. The v' profiles of Fig. 4(c) all show a slight increasing trend. A local peak is shown only for SWF2. The continuous increasing v' far downstream from the flame zone seems to be associated with slow precession of the flow, which is characteristic of open swirl flows.

Because the flames are axi-symmetric, the flame brush is locally normal to the incident centerline velocity vector. Further support of this notion is shown by the jpdf of Fig. 5 where the direction of flame-induced acceleration is parallel to U. Consequently, U(x) at the reactant boundary provides a convenient means to estimate the flame speed, S_f, as in the stagnation flow stabilized flames. Shown in Table I is the estimated S_f normalized by the corresponding laminar flame speed, S_l. These results show an almost linear dependence of S_f/S_l on u'/S_l and are in good agreement with results measured in other configuration[15].

The two-dimensional flowlines obtained in SWF1 and SWF4 and their corresponding non-reacting flowlines are compared in Fig. 6. Flowline tracing is appropriate because there is very little effect of swirl in the flame zones and in most of the surrounding co-flow. Also shown are the c contours deduced from MSOD which mark the time-averaged mean flame brush position. The planar SWF1 flame brush appears to be thicker than the curved SWF4 flame brush because of bouncing. The flowlines of SWF1 and Flow 1 are not significantly different. More differences are found between SWF4 and Flow 2 where SWF4 flowlines asymmetry and reduced divergence in the products are shown. The reduction is consistent with the change in mean pressure gradient generated by the higher flow velocity. Upstream of the reaction zone, the reacting and non-reacting flowlines are identical. The general features of the flowlines and flame shape of SWF4 and of other flames studied here resemble those of a stagnation point stoichiometric ethylene/air flame (S9 of reference 14) which was deemed as one of the closest approximations to a one-dimensional normal planar premixed turbulent flame. The S9 type flowfield, however, is achievable in the stagnation flow configuration only for a single mixture. The swirl stabilized flame configuration, on the other hand, is capable of producing similar flame flowfields under a much wider range of conditions.

Our results clearly show that flow divergence is the key flame stabilization mechanism. The main function of the weak swirl is to induce radial mean pressure gradients which cause flow divergence but not recirculation. The flame stabilizes itself at the position where mass flux equals the burning rate. Varying swirl changes the rate of divergence and causes the flame brush to reposition itself. Although the stagnation flow also stabilizes the flame by flow divergence, there are many differences between the two configurations. The swirl-stabilized flame zone is not in physical contact with any surfaces, thus avoiding downstream heat loss or flame interaction with the plate. For example, the stagnation flow configuration is not capable of supporting the lean condition of SWF2 because of wall interaction[14]. Flow divergence throughout the swirl generated flow is much smaller than in the stagnation flow. Moreover, it is much more convenient to adjust swirl than to adjust the stagnation plate separation distance to achieve the desire condition. This flame configuration is therefore by far the best for investigating fundamental properties of premixed turbulent flames and will provide new opportunities for investigating flame propagation phenomena such as flame speed, flame generated turbulence, burning rates and extinction or local quenching by turbulence.

It has long been recognized that all laboratory flame configurations have some limitations. The rod-stabilizer of v-flames and the pilot flame of large Bunsen flames may influence the development of flame wrinkles. As mentioned above, under lean conditions the stagnation plate interacts with the flame and influences its propagation. These side effects have to be carefully considered in the analysis and interpretation of the results for comparison with the prediction of theoretical models. To circumvent some of these limitations, Kostiuk et al.[17] developed the opposed flow burner which produces twin interacting flames, and North and Santavicca[18] developed a pulsed-flame flow reactor which produces unsteady freely propagating flames. The trade-off for the former is that the flame interaction has to be considered in the analysis of the data. For the latter, the transient turbulent flowfield is difficult to characterize by point measurements.

The swirl-stabilized flames are freely propagating, yet stationary. The flame zone is easily accessible to point or two-dimensional laser diagnostics such as tomography and particle image velocimetry and to detailed probing by point methods. Except for flow divergence, there is no other inherent limitation. There are several refinements, however, which can be made to the present apparatus to reduce some of the flame asymmetries and damp flow perturbations. The installation of additional swirl injectors with variable injection angles would be most useful to ensure an axi-symmetric flowfield. More precise control of the swirl injectors would help damp perturbations associated with the high pressure air supply and may lead to the stabilization of planar freely propagating premixed laminar flames. These experiments using the improved system, the analysis of conditioned velocity statistics, characterization of incident turbulence length scales, flame wrinkled scales and burning rates are forthcoming.

Conclusions

A novel method has been developed for stabilizing freely propagating premixed turbulent flames by weak swirl. Under flow condition of Re = 40,000 and swirl number ranging

from 0.005 to 0.3, locally normal methane-air and ethylene-air flames are stabilized for lean ($\phi = 0.57$) to stoichiometric mixtures.

The flowfields for six reacting and non-reacting conditions with and without incident turbulence are investigated using two-component laser Doppler anemometry and Mie scattering from oil droplets techniques. The velocity profiles show that the flames are stabilized by swirl-induced flow divergence rather than by recirculation. The flame is maintained where the local mass flux equals the burning rate.

Using well established procedures for analyzing premixed turbulent flame data, the velocity statistics and the scalar properties are shown to be characteristics of wrinkled laminar flames. The flame zones are free of swirling motion, and the flame speeds can be estimated based on the centerline velocity vector, which is locally normal to the flame brush. The flowlines and the mean c contours show that the flame flowfields are the closest approximations, to date, to the normal one-dimensional planar premixed turbulent flames of many theoretical models. Our investigation strongly suggests that this new flame configuration is worthy of further development into one of the standard configurations for comparison between experimental and theoretical works.

Acknowledgements

The visit to LBL by CKC, KSL and WKC was supported by a Research and Development Grant from Hong Kong Polytechnic. This work was supported by the Director, Office of Energy Research, Office of Basic Energy Sciences, Chemical Sciences Division of the U. S. Department of Energy under Contract No. DE-AC-03-76SF00098. The authors would like to acknowledge Mr. Gary Hubbard for the computer controlled and data reduction software.

References

1. Beer J.M. and Chigier N.A. *Combustion Aerodynamics*, Applied Science Publications, London, 1972.

2. Syred, N. and Beer, J. M. : Combustion and Flame 23, 143 (1974).

3. Claypole T.C. and Syred N.: 18th Symposium (Int'l) on Combustion, p. 81, The Combustion Institute, 1981.

4. Starner, S. H. and Bilger, R. W.: 21st Symposium (Int'l) on Combustion, p. 1569, The Combustion Institute, 1986.

5. Feikema D., Chen R.H. and Driscoll J.F.: Combustion and Flame 80, 183 (1990).

6. Milosavljevic V.D., Taylor A.M.K.P. and Whitelaw J.H.: Combustion and Flame 80, 196 (1990).2

7. Fuji S., Eguchi K. and Gomi M.: AIAA Journal 19 , 11, 1438 (1981).

8. Gouldin, F. C., Depsky, J. S., and Lee S.-L.: AIAA Journal 23, 1, 95 (1985).

9. ABD Al-Messeeh, W. A., Bradley, D., Gaskell, P. H., and Lau, A. K. C.: 23rd Symposium (Int'l) on Combustion, p. 825, The Combustion Institute, 1990.

10. Edwards, C. F., and Rudoff, R. C.: 23rd Symposium (int'l) on Combustion, p. 1353, The Combustion Institute, 1990.

11. Yu, H. K., Chin, W. K., Lau, K. S., Chan, C. K., and Tse, C. S. "Swirl Flow Effect on Combustion Characteristics of Liquid Fuel Spray in Optical Access Laboratory Furnace," Paper 90-32 Fall Meeting 1990 of the Western States Section Meeting of the Combustion Institute, Oct. 1990.

12. Cheng R.K. and Shepherd I.G.: Combustion and Flame 85, 7 (1991).

13. Cheng R.K. and Ng T.T.: Combustion and Flame 52 , 185 (1983).

14. Cheng. R. K., Shepherd, I. G., and Talbot, L.: 22nd Symposium (Int'l) on Combustion, p. 771 The Combustion Institute 1988.

15. Cho, P., Law, C. K., Hertzberg, J. R. and Cheng, R. K.: 21st Symposium (Int'l) on Combustion, p. 1493, The Combustion Institute, 1986.

16. Cheng, R. K.: Combustion Science and Technology, 41, 109 (1984).

17. Kostiuk, L. W., Bray, K.N. C., Chew, T. C.: Comb. Sci. Tech, 64, 4, 233 (1989).

18. North G. L., and Santavicca, D. A.: Comb. Sci Tech, 72, 4, 215 (1990).

Figure Captions

Fig. 1 Premixed flames stabilized by swirl for conditions SWF1 and SWF2.

Fig. 2 Schematics of the experimental and diagnostics systems.

Fig. 3 Radial profiles of radial, V, and tangential, W, velocity components at 10 mm above burner exit.

Fig. 4 Centerline mean and rms velocity profiles.

Fig. 5 Contour plot of the joint probability density function of velocity fluctuations obtained at the centerline of SWF4 at x = 32 mm c = 0.55.

Fig. 6 Two-dimensional flowlines and flame boundaries for (a) SWF1 and (b) SWF4. The reacting flowlines are marked by symbols and the non-reacting flowlines are shown as chain dotted lines.

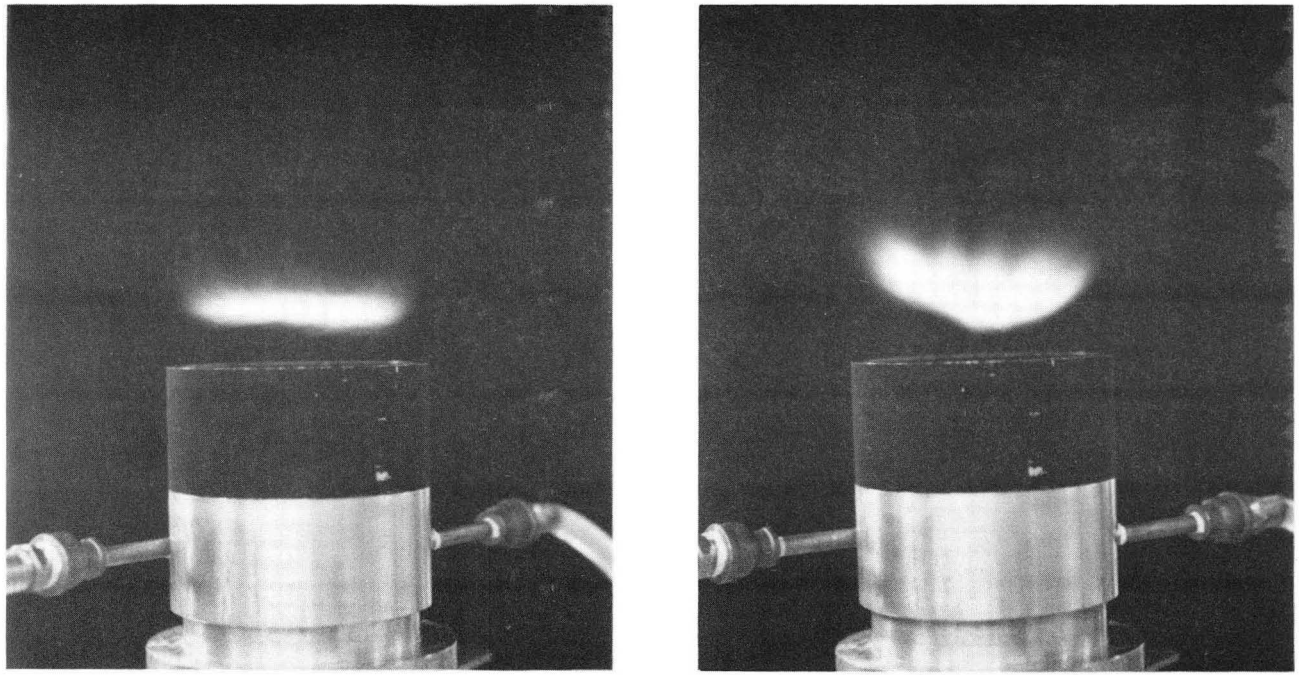

Fig. 1 Premixed flames stabilized by swirl for conditions SWF1 and SWF2.

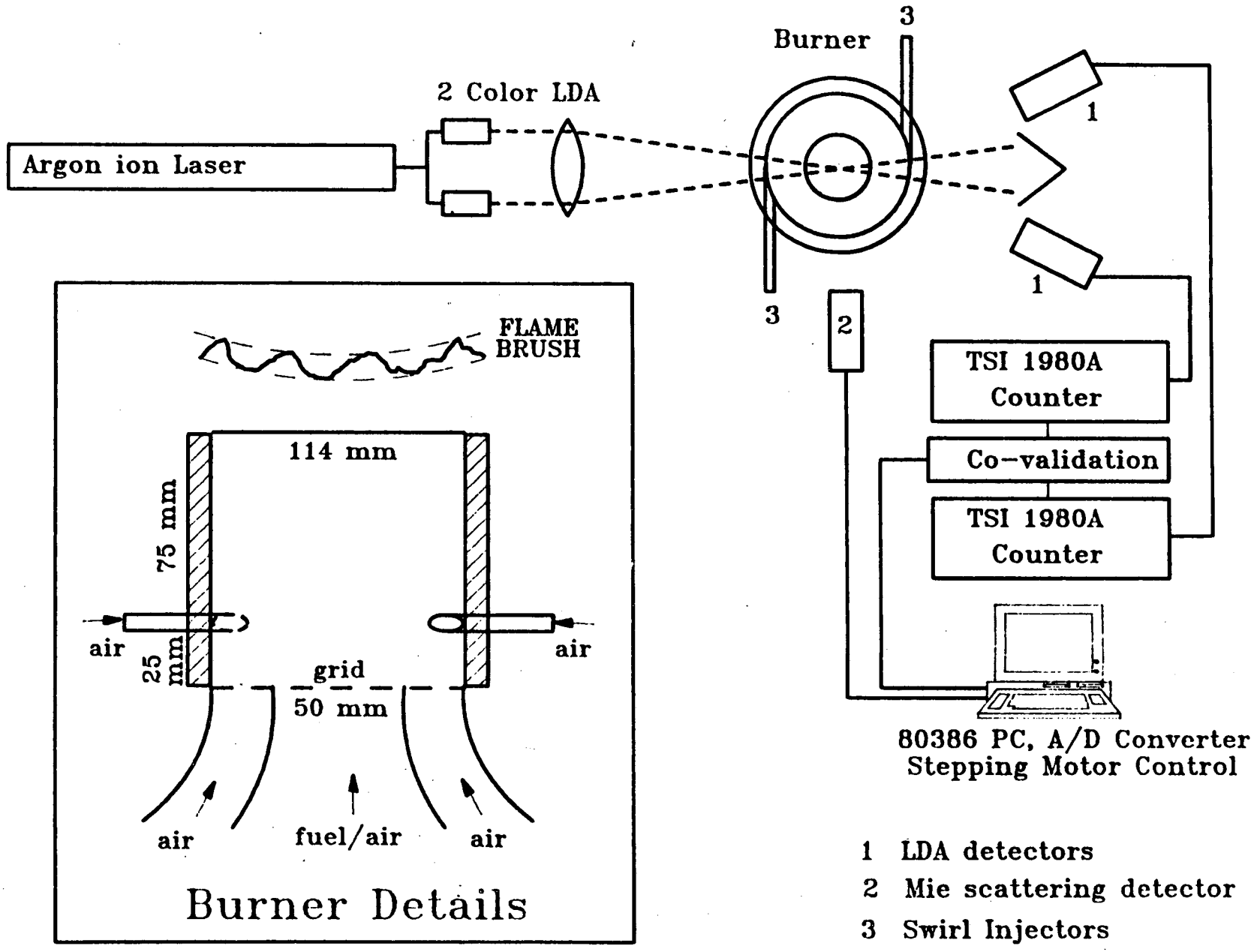

Fig. 2 Schematics of the experimental and diagnostics systems.

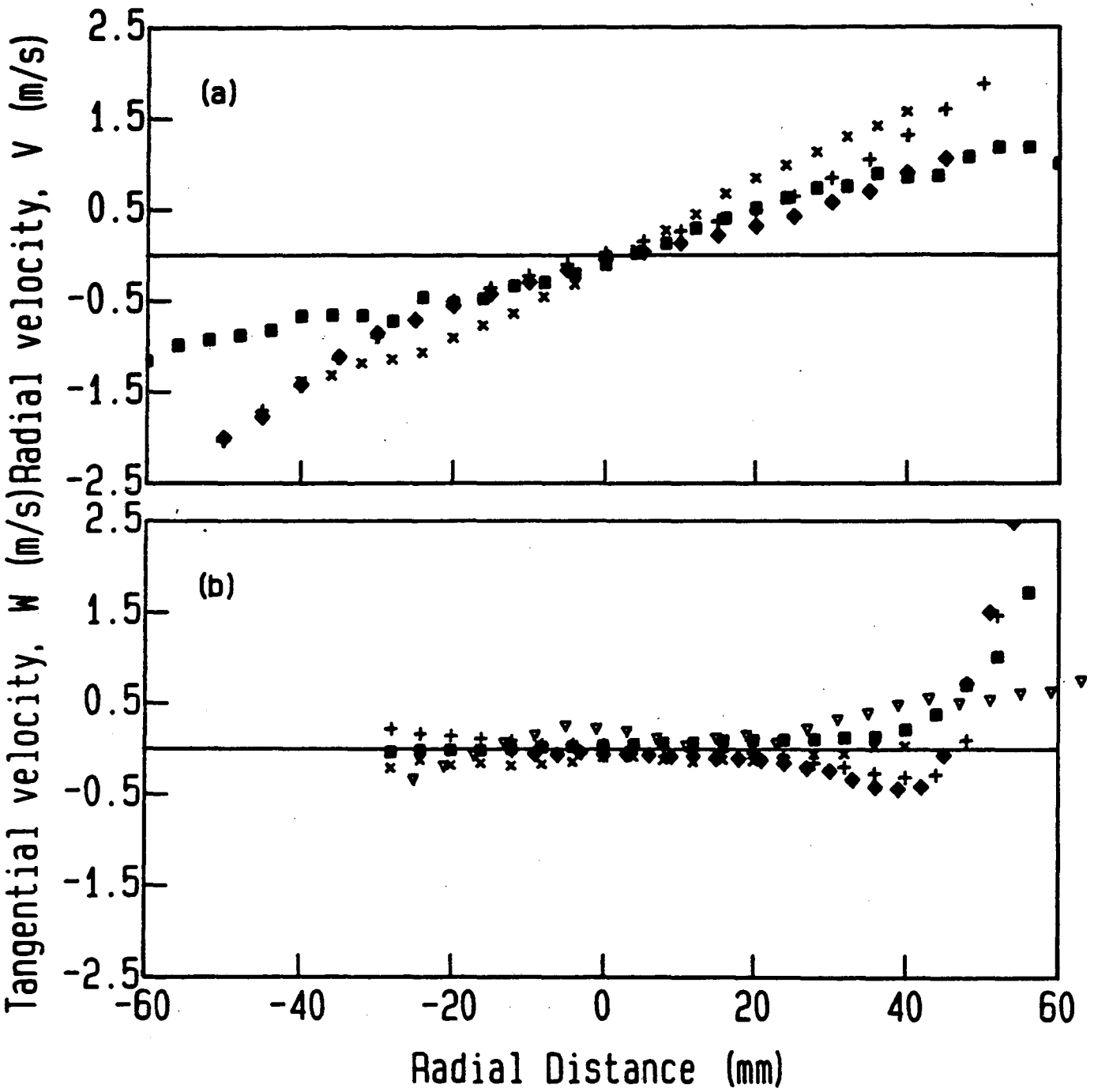

Fig. 3 Radial profiles of radial, V, and tangential, W, velocity components at 10 mm above burner exit.

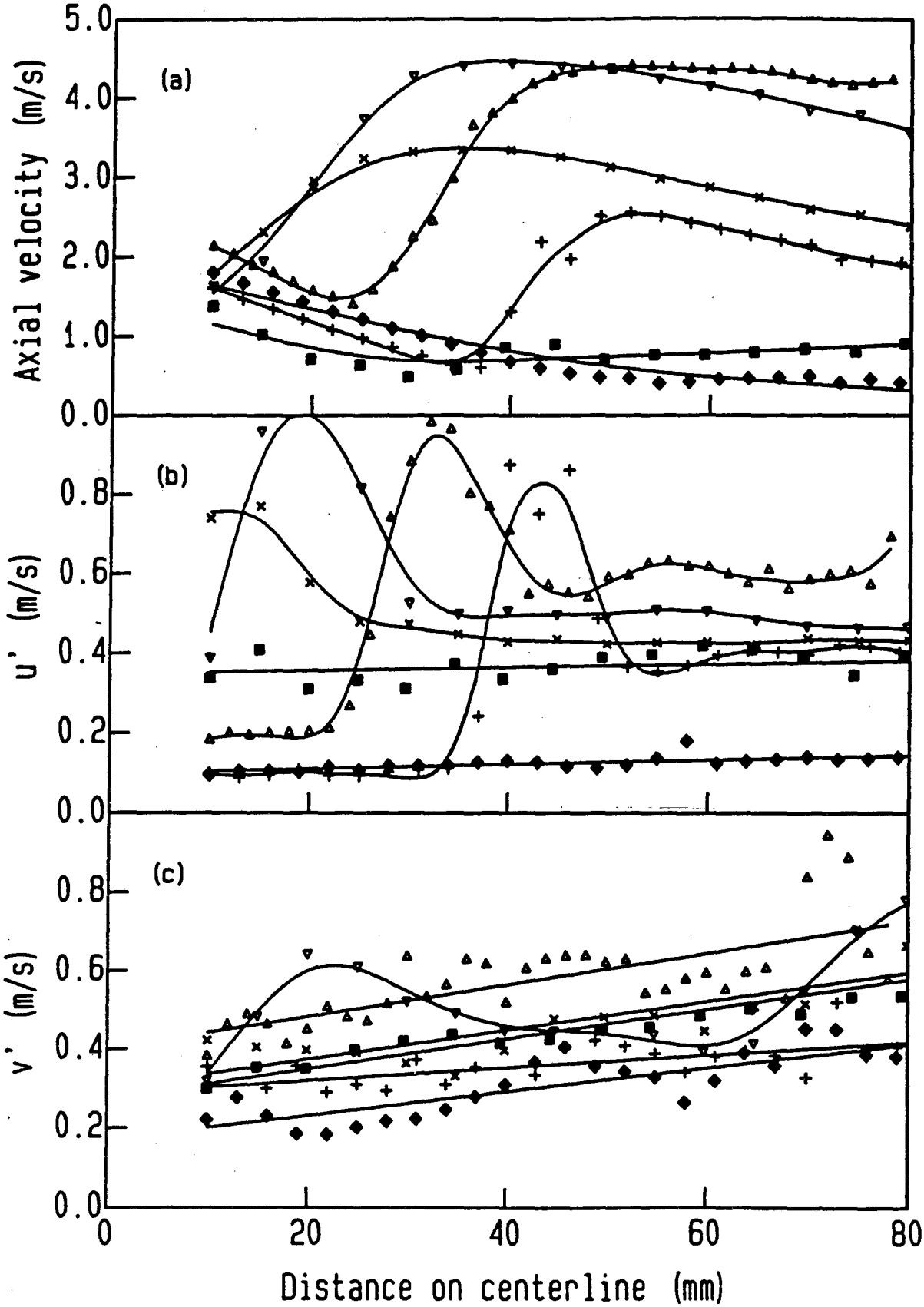

Fig. 4 Centerline mean and rms velocity profiles.

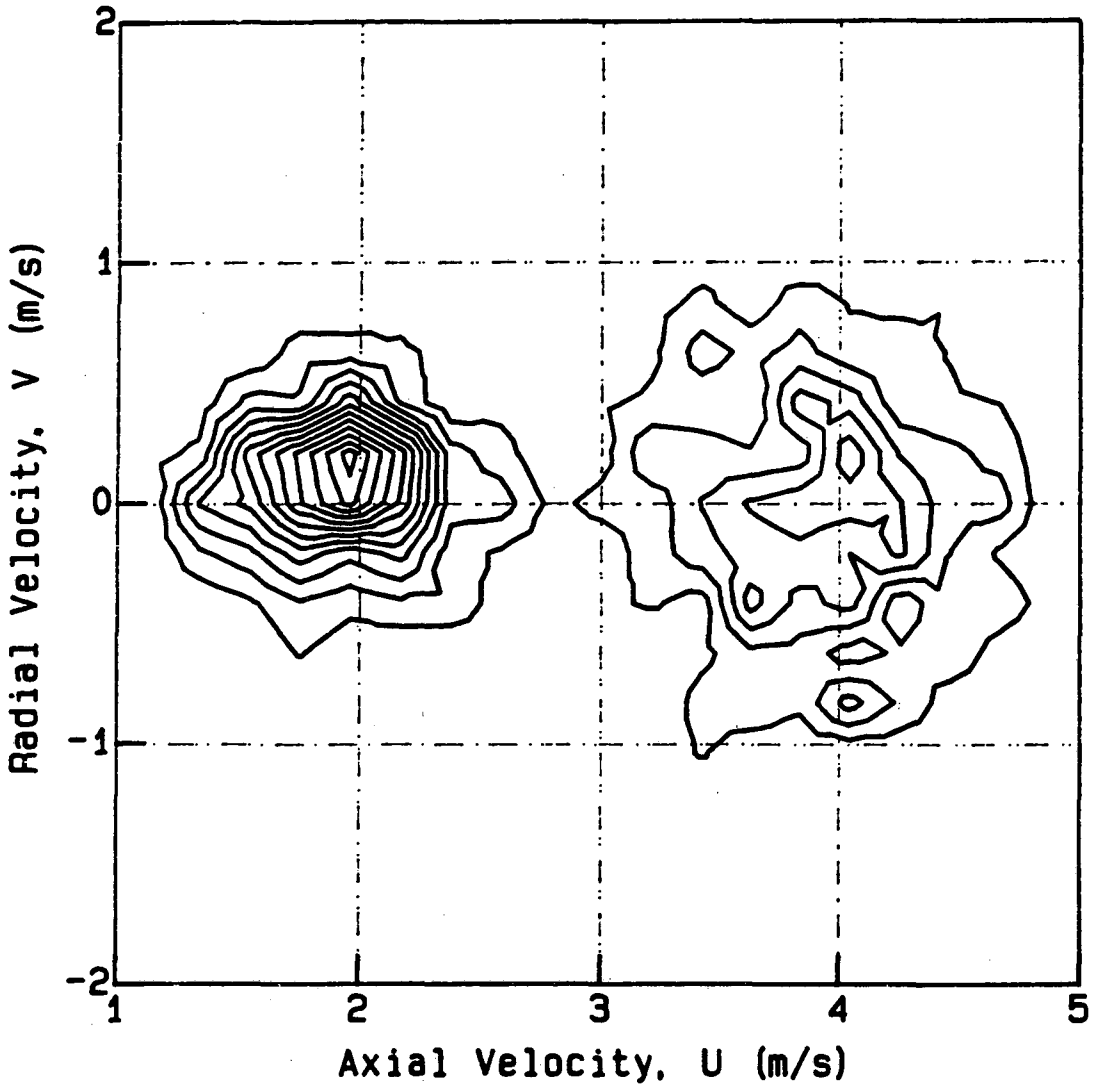

Fig. 5 Contour plot of the joint probability density function of velocity fluctuations obtained at the centerline of SWF4 at x = 32 mm c = 0.55.

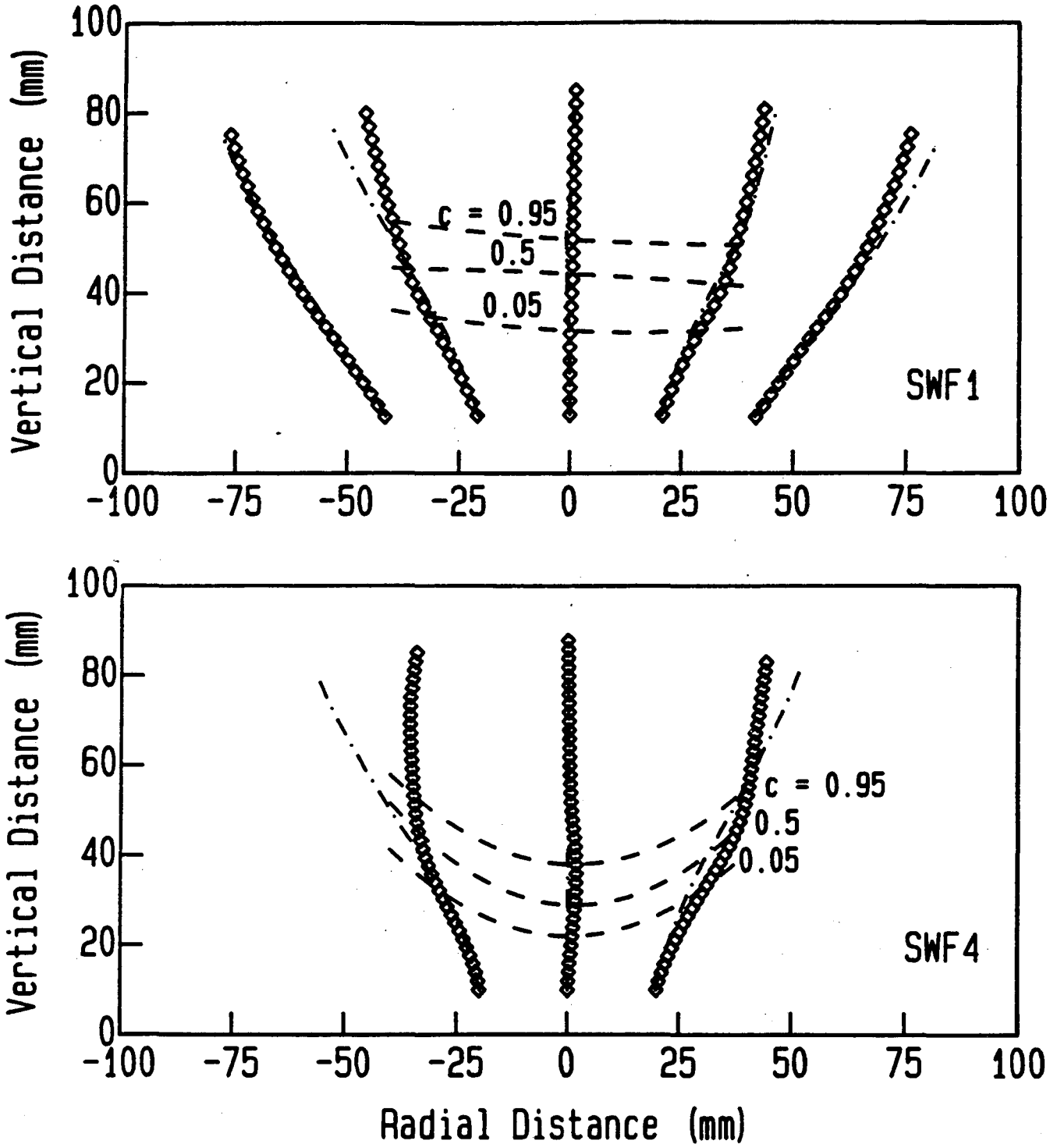

Fig. 6 Two-dimensional flowlines and flame boundaries for (a) SWF1 and (b) SWF4. The reacting flowlines are marked by symbols and the non-reacting flowlines are shown as chain dotted lines.

LAWRENCE BERKELEY LABORATORY
UNIVERSITY OF CALIFORNIA
TECHNICAL INFORMATION DEPARTMENT
BERKELEY, CALIFORNIA 94720